UNIVERSITY OF CRETE
FACULTY OF SCIENCE
DEPARTMENT OF BIOLOGY

Διατμηματικό Πρόγραμμα Μεταπτυχιακών Σπουδών : **ΜΟΡΙΑΚΗ ΒΙΟΛΟΓΙΑ-ΒΙΟΪΑΤΡΙΚΗ**

Μεταπτυχιακή Εργασία

ΤΑΥΤΟΠΟΙΗΣΗ ΕΝΖΥΜΩΝ ΑΠΟ ΨΥΧΡΟΦΙΛΑ ΒΑΚΤΗΡΙΑ ΜΕ ΠΙΘΑΝΕΣ ΕΦΑΡΜΟΓΕΣ ΣΤΗ ΒΙΟΤΕΧΝΟΛΟΓΙΑ

ΣΥΜΕΩΝΙΔΟΥ ΑΝΘΗ

ΕΠΙΣΤΗΜΟΝΙΚΟΣ ΥΠΕΥΘΥΝΟΣ:ΚΑΦΕΤΖΟΠΟΥΛΟΣ ΔΗΜΗΤΡΙΟΣ

ΣΕΠΤΕΜΒΡΙΟΣ 2016

Contents

Ευχαριστίες

Για την εκπόνηση αυτής της μικρής σε διάρκεια έρευνας, πολλές εργατοώρες «σπαταλήθηκαν» από άτομα διαφόρων κλάδων. Ένα μεγάλο «Ευχαριστώ» στον ανελλιπώς ενεργό επιβλέποντα μου Κουτσιούλη Δημήτρη για την εμπιστοσύνη που μου έδειξε καθώς και για την καθημερινή καθοδήγηση που μου έδινε. Θέλω να ευχαριστήσω επίσης, τον κ. Καφετζόπουλο Δημήτρη για την εμπιστοσύνη του προς το πρόσωπο μου και για όλες τις χρήσιμες συμβουλές και υποδείξεις καθ' όλη τη διάρκεια της εξέλιξης της διπλωματικής μου, καθώς και τον κ. Μπουριώτη Βασίλη για την προσφορά της βακτηριακής συλλογής του και τις συμβουλές του, για τον καλύτερο χειρισμό των πειραμάτων.

Φυσικά, θα ήθελα να ευχαριστήσω το δεξί μου χέρι που για καλή μου τύχη δεν ήταν ένα, αλλά πέντε!! Χαρά Γ. , Χρυσούλα Β. , κ. Δημήτρη Δ., Δέσποινα Β. και Παντελή Τ. σας ευχαριστώ όλους από καρδιάς για τη βοήθεια, τις συμβουλές και τις υποδείξεις σας, μα πάνω απ' όλα για την προθυμία σας να με βοηθήσετε, οποιαδήποτε στιγμή και αν σας χρειάστηκα.

Περίληψη

Τα κρύα ενδιαιτήματα αποικίζονται από ψυχρόφιλους οργανισμούς που ανέπτυξαν ποικίλους μηχανισμούς προσαρμογής σε χαμηλή θερμοκρασία, ένας από αυτούς εστιάζεται στις τροποποιήσεις των ενζύμων τους. Περαιτέρω έρευνες σε ψυχρόφιλα ένζυμα θα μπορούσαν να οδηγήσουν σε καλύτερη κατανόηση των μηχανισμών προσαρμογής τους σε αυτές τις συνθήκες και να αξιολογήσουν την πιθανή εφαρμογή τους στη βιοτεχνολογία, εξαιτίας της υψηλής δραστικότητας σε χαμηλές θερμοκρασίες και της εύκολης απενεργοποίησης τους με θερμική επώαση .

Σε μια συλλογή από ~262 ψυχρόφιλα/ψυχρότροφα βακτηριακά στελέχη από την Ανταρκτική, πραγματοποιήθηκε σάρωση για την ύπαρξη δυο ενζυμικών ενεργοτήτων: νουκλεάσης και αλκαλικής φωσφατάσης. Ακολούθησε γενωμική αλληλούχιση των στελεχών με τα πιο επιθυμητά χαρακτηριστικά και ταυτοποίηση των αλληλουχιών που κωδικοποιούν τα επιλεγμένα ένζυμα.

Ένα γονίδιο από το βακτηριακό στέλεχος TAB110α, που φέρεται να κωδικοποιεί μια αλκαλική φωσφατάση, παρουσιάζει ~75% και 30% ταυτοποίηση με τις αμινοξικές αλληλουχίες της *E.coli* (ECAP) και Ανταρκτικής (AnP) αλκαλικής φωσφατάσης, αντίστοιχα.

Κλωνοποίηση του γονιδίου σε pRSETB φορέα και ετερόλογη έκφραση σε *E.coli* στέλεχος έκφρασης, απέδωσε πρωτεΐνη με 70-80%% καθαρότητα.

Περαιτέρω πειράματα, σχετικά με την καταλυτική αποδοτικότητα και την θερμική αστάθεια του ενζύμου, θα μπορούσαν να διαλευκάνουν τον δυνητικά ψυχρόφιλο χαρακτήρα του. Χρησιμοποιώντας ένα φυσικό υπόστρωμα, όπως πλασμιδιακό DNA, η αποδοτικότητα της αποφωσφορυλίωσης του θα μπορούσε να μετρηθεί και να συγκριθεί με άλλες εμπορικές αλκαλικές φωσφατάσες προκειμένου να διευκρινιστεί η πιθανή χρήση του σε εφαρμογές μοριακής βιολογίας.

Abstract

Cold environments are colonized by psychrophiles, organisms that developed adaptation mechanisms in low temperature through their enzymes, the prerequisite to the environmental adaptation. Further investigations in psychrophilic enzymes could lead to better understanding of adaptation mechanisms and evaluate their potential application in biotechnology due to their high activity in low temperature and heat lability.

Possessing an Antarctic psychrophilic/psychrotolerant bacterial strain collection, consisting by 262 strains, a high-throughput screening for DNase and alkaline phosphatase activity was carried out followed by DNA sequencing of the most desirable strains. Furthermore, sequences coding for the target enzymes were identified.

A gene from TAB110a strain encoding an alkaline phosphatase, displays ~75% and ~30% identity with ECAP and AnP, respectively. Successful cloning of this gene into the pRSETB plasmid and heterologous expression in an *E.coli* strain yielded protein with 70-80% purity.

Further experiments on the catalytic efficiency and heat resistance, could elucidate its putative psychrophilic character. Using a native substrate, like a plasmid DNA, dephosphorylation efficiency could be measured and correlated with other commercial APs in order to determine its potential use in molecular biology applications.

Introduction

1. The life in cold environments

One of the most widespread natural stress parameter on Earth is the low temperature. Due to the fact that 70% of our planet surface is covered by oceans, 90% of them have a temperature close to or below 5^{o}C in a big depth. The majority of terrestrial habitats that are permanently cold are located in Alaska, Canada, Russia, China and Antarctica. Permafrost habitats, like Polar Regions, glacier and alpine regions, constitute 20% of terrestrial soils (Rodrigues and Tiedje, 2008).

Although, these habitats are inhospitable and frigid for many of the familiar species, as well as the human being, cold-adapted organisms are colonized there. Understanding the mechanisms of adaptation of these organisms may accommodate basic principles of adaptation and serves the opportunity to search for life on other planets. Microorganisms that live in these habitats are the most successful colonizers (Rodrigues and Tiedje, 2008).

Psychrophiles are the organisms that live in these cold environments. Based on the ambiguous Morita's definition, these organisms have optimum growth temperature of <15^{o}C and a maximal temperature for growth at about ~20^{o}C (Morita, 1975). New terms, such as stenothermal (obligate psychrophiles) and eurythermal (facultative psychrophiles) organisms have been proposed, in order to take into account the arbitrariness in the growth temperature range of Morita's definition (Feller and Gerday, 2003). Psychrophiles consist of all three domains: *Bacteria*, *Archaea* and *Eukarya*. They most abundant representatives are bacteria (i.e. *Pseudoalteromonas, Moraxella, Psychrobacter, Pseudomonas, Polaribacter, Arthrobacter* and *Bacillus* species), yeast (*Candida* and *Cryptococcus* species), algae (Chloromonas), archaea (*Methanogenium*, *Methanococcoides* and *Halorubrum* species), plants and animals (Morita, 1975; Gounot, 1991; Cavicchioli, 2006; Morgan-Kiss *et al.*, 2006; Margesin *et al.*, 2007; Buzzini *et*

al., 2012). All these examples illustrate the abundance of psychrophiles in terms of diversity and distribution (Feller, 2013).

They do not simply survive in such extreme environments, but they bear a wide range of adaptive features at all levels of the cell architecture and function. Psychrophiles have some severe physicochemical constraints to deal with such as increased water viscosity, reduced biochemical reaction rates, perturbation of weak interactions driving molecular recognition and interaction, strengthening of hydrogen bonds, reduced fluidity of cellular membranes etc (Rodrigues and Tiedje, 2008; Feller, 2013). Adaptive features can be detected in the genome sequence of psychrophilic organisms and high throughput approaches could further introduce new data (Medigue *et al.*, 2005; Bowman, 2008). These adaptations include mechanisms of freeze tolerance or avoidance, maintenance of proteins synthesis, production of cold-acclimation proteins and regulation of membrane fluidity (Feller and Gerday, 2003).

2. Psychrophilic enzymes and mechanisms of adaptation

The key to adaptation in cold environment lies in the protein function and especially in enzymes, which are considered the prerequisite to the environmental adaptation. They exhibit high activity at low temperatures in order to face the exponential decrease in chemical reaction rates (Feller, 2013).

A study *on Pseudoalteromonas haloplanktis* showed that 30% of the upregulated proteins at 4^{o}C were found related with protein synthesis, suggesting that protein synthesis may be a rate-limiting step for growth in the cold and by inducing it gives a compensatory cellular response (Piette *et al.*, 2010). High expression levels of ribosomal proteins, chaperones, such as TF (a cold shock protein in *E.coli*), and DNA helicases, high number of rRNA genes and tRNA genes, were observed in different organisms, claiming the need for high capacity and efficiency for translation in the cold (Medigue *et al.*, 2005; Jung *et al.*, 2010; Piette *et al.*, 2010; Feller, 2013). Another strategy for the adaptation of psychrophiles in the cold, is the reduction of proline content in protein sequences in order to overcome the proline isomerization, a rate-

limiting step for the folding of the most proteins(Feller and Gerday, 2003; Baldwin, 2008).

Furthermore, other adaptation strategies of psychrophiles are connected with enzyme activity. Cold active enzymes bear discrete changes on their 3D structure compared to mesophilic counterparts, which are responsible for their psychrophilic character. Changes in their kinetic parameters, (k_{cat} and K_m) correspond to their high activity and flexibility at low temperatures. Most of the cold active enzymes improve their k_{cat} value at the expense of K_m (Feller and Gerday, 2003; Feller, 2013). Due to the weaker affinity to their substrate, their free energy of activation *Δ*G is lower in correlation with their mesophilic and thermophilic counterparts (Figure 1), that occasionally comes from lower enthalpy and entropy, the two components of *Δ*G; therefore their activity is increased (D'Amico, Marx, *et al.*, 2003) . This thermodynamic link between affinity and activity seems to improve the activity at low temperatures in many cold active enzymes (Fields and Somero, 1998).

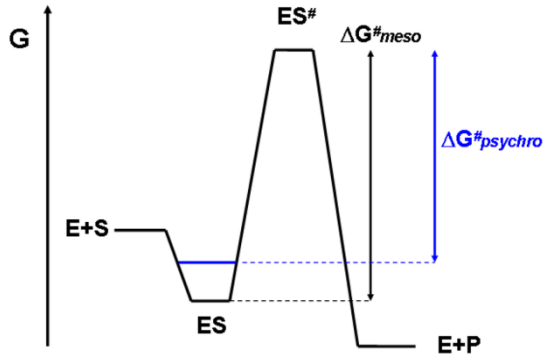

Figure 1: Weak substrate binding (blue) decreases the activation energy (ΔG# psychro) and thereby increases the reaction rate (Feller and Gerday, 1997)**.**

Others characteristics to render them adapted to cold temperatures, is the higher heat-liability of their active site than the whole protein structure, which is consistent to their flexibility (Fields and Somero, 1998; Collins *et al.*, 2003). Based on crystal and X-ray structures of a cold active *α*-amylase, the basic observation was that the amino acid composition of its catalytic cleft is strictly conserved correlated to its mesophilic structural homologue (Aghajari *et al.*, 1998). Nonetheless, alterations on the active site structure in other cases were observed. These alterations facilitate better accessibility, which

means lower energy cost and comprise replacement of bulky side chains for small groups, distinct conformation of the loops bordering the active site and additional metal binding sites (Aghajari *et al.*, 2003; Bjelic *et al.*, 2008; Jung *et al.*, 2008). Differences in electrostatic potentials near the active site region and improvement of their dynamics appear to facilitate their binding with substrate and be also a significant parameter for activity at low temperatures (Smalas *et al.*, 2000). Alterations to the interaction nature between the cold active enzymes and substrates, from hydrophobic to electrostatic, can further enhance their interaction at low temperatures (Lonhienne *et al.*, 2001).

Comparative microcalorimetric studies in psychrophilic and mesophilic enzymes revealed that psychrophilic structures are stabilized by few weaker interactions. As a result disrupting only some of them lead to unfolding. Additionally, a reversible character of psychrophiles' unfolding is remarkable, owing to the weakening of hydrophobic bonds of the core clusters in contrast to the irreversibility of unfolded structure of mesophilic enzymes (Georlette *et al.*, 2003; Feller, 2013). Generally, different combinations of alterations to structural factors known to stabilize the protein molecule are observed in psychrophilic enzymes structure. Some determinants are, glycine residues providing local mobility (Mavromatis *et al.*, 2002), attenuation of proline residues in loops that enhance flexibility between secondary structure (Sakaguchi *et al.*, 2006), attenuation of salt bridges and H-bonds due to the reduction of arginine residues (Siddiqui *et al.*, 2006), lower number of ion pairs and aromatic interactions (Smalås *et al.*, 1994), smaller size and relative hydrophobicity of nonpolar residue clusters in protein core (Saelensminde *et al.*, 2009), larger cavity size (Paredes *et al.*, 2011), weaker binding of stabilizing ions (Ca^{+2}) (Feller *et al.*, 1994), insertions and deletions of extrasurface charges and weakness of subunit interactions respectively (Rentier-Delrue *et al.*, 1993; Davail *et al.*, 1994), lack of disulfide bonds (Feller *et al.*, 1994), higher proportion of nonpolar residues to the surrounding medium (Georlette *et al.*, 2003), an excess of negative charges at the surface of the protein that corresponds to a more acidic pI than their mesophilic and thermophilic homologues (Feller *et al.*, 1999).

There are no general rules about the combination and number of the above-mentioned factors that define the mobility of psychrophilic enzymes (Feller, 2013). However, some common features that appear at a lower percentage for enzymes that exhibit decreased optimal temperatures are: the number of ion pairs, the side-chain contribution to the exposed surface, and the polar regions in the buried surface (Gianese *et al.*, 2002).

Comparative experimental insights between a psychrophilic *α*-amylase and engineered mutants revealed that the disappearance of stabilizing interactions in psychrophilic enzymes increases the flexibility of catalysis and the dynamics of active site residues at low temperatures, leading to a higher activity (D'Amico, Gerday, *et al.*, 2003; Papaleo *et al.*, 2011; Feller, 2013).

From an evolution point of view, directed evolution and protein engineering experiments of psychrophilic enzymes revealed that there is no physical link between activity and stability, but they are usually connected due to their simultaneous appearance. It is believed that high activity at low temperature can be associated with the lack of selection pressure for stability and is considered as the simplest adaptive strategy for enzymatic catalysis in the cold (Giver *et al.*, 1998; Wintrode and Arnold, 2000; Feller, 2013). This relationship between activity-flexibility-stability is depicted in energy landscapes called folding funnel model for psychrophiles and thermophiles, based on physical and biochemical data available for them, describing all the folding-unfolding interactions (Figure 2) (Schultz, 2000).

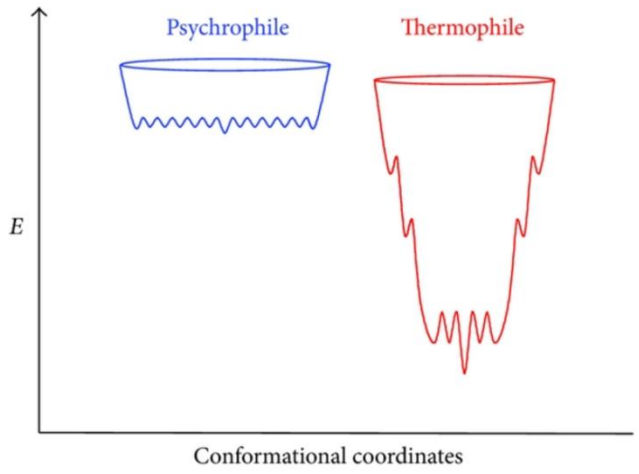

Figure 2: Folding funnel model of enzyme temperature adaptation. Characteristics depiction. The free energy of folding (E): function of the conformational diversity, Height: the determination of the conformational stabilities. Top: the unfolded states in the numerous random coil conformations. Bottom: the native and catalytically active conformations. Ruggedness of the bottom: the energy barriers for interconversion, or structural fluctuations of the native state (Schultz, 2000)**.**

Most enzymes from psychrophiles have biotechnological applications due to four main advantages: they have high activity and lower concentration is needed for the catalysis, they remain active at tap water and ambient temperature avoiding heating during the process, they are heat labile, therefore moderate temperature and less energy cost is needed for inactivation and they are adapted to various environmental constraints (Feller, 2013; Sarmiento *et al.*, 2015).

3. Alkaline phosphatases

Alkaline phosphatases (APs, EC 3.1.3.1) are widely distributed in nature and exist from bacteria to human (McComb *et al.*, 1979). With few exceptions, they create homodimers and their catalytic site bears three metal ions necessary for their enzymatic activity, two Zn^{2+} and one Mg^{2+}. They hydrolyze phosphoric esters and catalyze a transphosphorylation reaction in the presence of large concentrations of phosphate acceptors with higher efficiency in basic (alkaline) pH values. Some suitable substrates for these enzymes are nucleic acids, proteins and alkaloids.

In Gram-negative bacteria, alkaline phosphatase is located to the periplasmic space and is considered to have a crucial role in the establishment of an increasing rate of diffusion of the molecules into the cells with simultaneous avoidance of them to diffusing out, through dephosphorylation (Horiuchi *et al.*, 1959). Dephosphorylation may be important for bacterial uptake of organic compounds.

Comparative studies, both in amino acid sequence and protein structure, indicated conservation of the functionally significant residues (Hulett *et al.*, 1991). Despite of the high conservation of catalytic mechanism between mammalian and bacterial alkaline phosphatases, they display significant differences: mammalian APs have higher specific activity, lower heat stability and need a more alkaline pH value for their activity than their bacterial counterparts (Murphy and Kantrowitz, 1994). Two significant alterations to residues close to the active site of *E.coli* AP (ECAP) are observed in correlation with mammalian alkaline phosphatases. Amino acid substitution of one of them leads to a mutant ECAP with mammalian alkaline phosphatase characteristics (Murphy *et al.*, 1993).

The structure of an alkaline phosphatase (TAP) which was isolated from the Antarctic strain TAB5, was compared with ECAP and conservation in almost all of the crucial residues at the active site was observed, with the addition of two new magnesium ions outside of the active site, which may be correlated with the substrate binding and local stability. TAP structure bears the typical cold adapted enzymes features, such as lack of disulfide bridges, low number of salt bridges, glycine clusters and a loose dimer interface that completely lacks charged interactions (Figure 3) (Rina *et al.*, 2000; Wang *et al.*, 2007). These features agree with TAP high catalytic activity at low temperatures and relative instability at high temperatures. A study using directed evolution identified the key residues that are responsible for the enzyme's cold-adapted activity and stability (Koutsioulis *et al.*, 2008). Comparisons between the wild type and mutants APs revealed that there is a subtle balance between the enzyme activity and stability and that it is possible to achieve a simultaneous improvement of these two characteristics through directed evolution (Koutsioulis *et al.*, 2008).

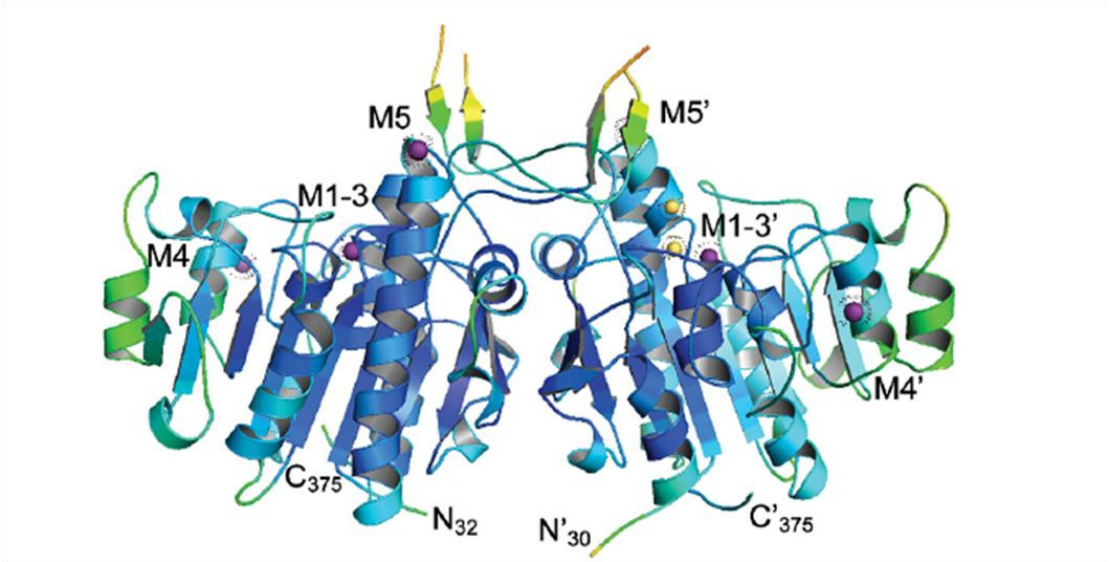

Figure 3: Side-view of the overall structure of TAP. Zinc ions are yellow and Magnesium ions are magenta. N terminus, C terminus and the metal-binding sites are indicated (M1-3', M4', M5') (Wang *et al.*, 2007)**.**

Alkaline phosphatase is useful in molecular biology, especially, in cloning procedures, since it removes the phosphate groups on the 5' end of DNA, preventing it from ligating, therefore keeping it linear until the following procedure. Additionally, removal of phosphate groups allows the replacement by radioactive phosphate groups when labeled DNA needs to be measured. An additional application is in enzyme immunoassay (ELISA).

4. Nucleases

Nucleases are enzymes that belong to esteraces (EC 3.1), a subgroup of hydrolases. They cleave the phosphodiester bonds of nucleic acids and it is difficult to be classified due to the high variation of their characteristics.

Based on their substrate preference, they can be divided into DNases, RNases and RNA/DNA nucleases (Hsia *et al*., 2005). Depending on whether a 5' or 3' end is needed for substrate recognition and whether cleavage products are single or oligo nucleotides, they can be separated in exo- and endonucleases (Figure 4).

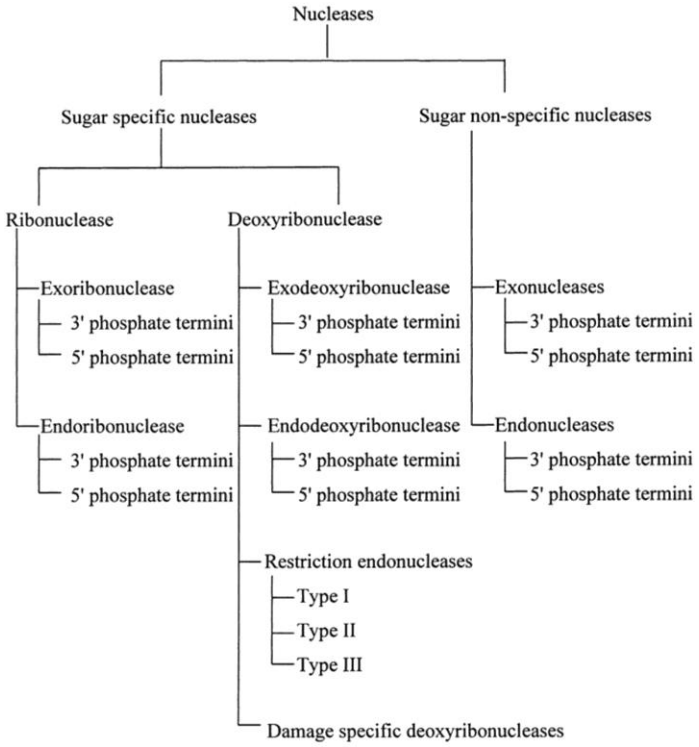

Figure 4: Schematic representation of the classification of nucleases (Linn *et al.*, 1982)**.**

Corresponding to the metal ion as a part of the catalytic mechanism, they can be divided in three classes, two-metal-ion-dependent, one-metal-ion-dependent and metal-independent nucleases. Two-metal-ion-dependent nucleases comprise the largest number of different tertiary folds and mediate the most diverse set of biological functions (Yang, 2011). Mg^{2+} ion is most frequently associated with nucleic acid enzymes (Cowan, 2002). This frequent use of Mg^{2+} is perhaps because of its abundance, solubility, redox stability when compared with Mn^{2+}, Fe^{2+} and Cu^{2+}, its small size relative to Ca^{2+}, and its rigid coordination geometry when compared with the transition metals Fe^{2+}, Cu^{2+}, Ni^{2+} and Zn^{2+} (Cowan, 2002; Maguire and Cowan, 2002; Yang, 2011).

Two well-known examples of psychrophilic nucleases applicable to molecular biology are the following: a) shrimp nuclease, isolated from shrimp *Pandalus borealis*, is a psychrophilic enzyme, which selectively degrades double-stranded DNA. It is used in molecular biology for removal of DNA contaminants in PCR mixtures or RNA preparations and its heat inactivation occurs at $55^{o}C$ before the addition of the template to the reaction. Recombinant and engineered forms are also performed (Sandsdalen *et al.*, 2003). b) Cryonase, a non-specific nuclease (can digest single-stranded,

double-stranded, linear or circularized DNA or RNA). It was isolated from the psychrophilic strain *Shewanella frigidimarina* and is active even when samples are on ice. A recombinant form is offered by Takara-Clontech (Cootes *et al.*, 2009).

Aim

Characterization of psychrophilic enzymes is essential in the elucidation of cold adaptation mechanisms. Furthermore, due to their special characteristics, like their high activity in a lower concentration in ambient temperature, their heat lability character and their adaptation to diverse environmental constraints possess an important role in biotechnology and industry. Consequently, further experimentation and investigation of them could lead to more promising psychrophilic enzymes with biotechnological applications.

A psychrophilic/psychrotolerant bacterial strain collection, consisting of 262 strains will be studied for the identification of novel cold-adapted enzymes with potential applications in biotechnology.

Materials and Methods

1. Cell cultures and conditions

In order to identify the viability of the chilled psychrophilic strains, 2μl from each glycerol stock were plated on LB agar plates (5g yeast extract, 10g tryptone, 5g NaCl and 15g agar per Liter) for 72h at 8^{o}C. New cell glycerol stocks were used to the following experiments.

2. DNase activity

For the determination of the DNase activity of psychrophilic strains, a method was performed using DNase test agar-methyl green broth with pH 7.3. An amount of 0.05g methyl green (as indicator for nuclease activity, SigmaAldrich) was added at 1L of LB agar broth. 2μl from each new cell glycerol stock were plated on to DNase test agar-methyl green plates at 8^{o}C. The DNase activity was estimated based on the extent of the visible ring (due to the hydrolyzation of the DNA) around the colonies after 5 days incubation. A manual counting scale was created from 0 to 2 in order to determine the size of the visible ring. A dash was used for the non-viable strains.

A second method was developed for the determination of DNase activity based on digestion of DNA. For this reason, 2μl of each strain were cultures in 750μl liquid LB at 8^{o}C for 48h. The viable strains, based on their A_{600} measurement, followed by cell disruption (30" sonication, intervals on ice) were used for the digestion test. 10μl from each sample were used in a reaction containing 0.5μg λDNA and 1X nuclease buffer (10mM Tris-HCl pH7.9, 10mM $MgCl_2$, 10mM NaCl) in an overnight incubation at 8^{o}C. Heat inactivation (at 65^{o}C for 10 min) was performed in the same samples and they were also tested for their DNase activity based on the abovementioned reaction conditions. The efficiency of the λDNA digestion was estimated by analyzing samples before and after heat treatment in1% agarose gel electrophoresis. A measuring scale, based on the grade of DNase activity, was created with the following characterization, "no", "low", "medium", "high" and "super high". The "no", "medium" and "good" characterizations refer to the level of DNase activity after the heat inactivation. Samples without DNase

activity didn't continue for the heat inactivation test and are represented as a dash (-).

3. Alkaline phosphatase activity

Alkaline phosphatase activity was determined by the *p*NPP assay in disrupted cells, as prepared in the DNase activity assay. Heat inactivation was also performed for 10 min at 65^{o}C. Each reaction consisted of 10μl of each cell sample, 10μl 10X phosphatase buffer (10mM $MgCl_2$, 1mM $ZnCl_2$ and 500mM BIS-TRIS propane pH 7) and 80μl of 5mM *p*NPP substrate at 8^{o}C for 2 days. The amount of the released product (4-Nitrophenol) was measured by absorbance at 405nm in a spectrophotometer (Fluostar Galaxy) (Figure 5).

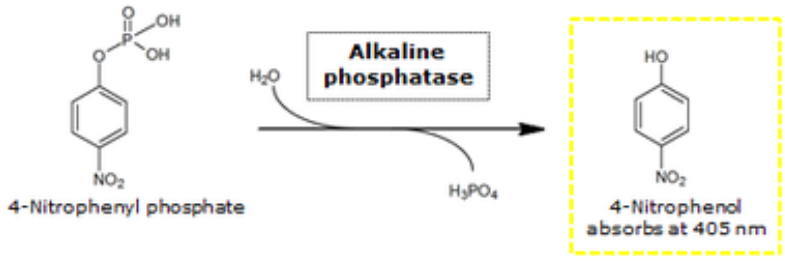

Figure 5: Hydrolysis of *p*NPP to yellow 4-Nitrophenol by alkaline phosphatase.

4. Sequencing and annotation

DNA of nine strains with selected characteristics (based on manual selection) was sequenced. DNA extraction was performed in liquid LB cultures (for 48h at 8^{o}C) after a triple cell streaking. DNA was extracted from 2 x 10^9 cells (A_{600}) using the PureLink Genomic DNA Mini kit (Invitrogen).

DNA sequencing (by Genomics Facility, IMBB)

Bacterial DNA was quantified using Qubit. Library was prepared using the Ion Xpress Plus Fragment Library kit, according to the manufacturer's instructions. Briefly, 100 ng DNA were subjected to shearing using Fragment Ion shear plus reagents. Sheared DNA was purified with Agencourt AmpPure XP kit followed by adapter and barcode ligation and nick repair. Adapter-ligated and nick-translated DNA was purified and size selected with e-gel (Invitrogen). The target peak size of the unamplified library was ~270 bp. The unamplified size-selected library was PCR amplified and purified before

template preparation (Ion PI Hi-Q OT2 200 kit) and Ion Torrent semiconductor sequencing (Ion PI Hi-Q sequencing 200 kit) using the Proton platform (PI chip). In total, 9 samples were loaded in one PI chip yielding 6M-11M reads per sample.

Annotation (by Bioinformatics Support Group, IMBB)

Due to the absence of a reference genome, *de novo* annotation was followed in order to determine the coding regions. MAKER platform (http://www.ncbi.nlm.nih.gov/pmc/articles/PMC2134774/) was used for this purpose with the results been blasted (both blastx and tblastn) versus the bacteria non redundant database of NCBI. In the case of the APT110a predicted peptide was checked for the presence of the appropriate motifs via FIMO (http://meme-suite.org/tools/fimo).

5. Selection of the desirable alkaline phosphatase gene

Annotation based on sequences of commercial alkaline phosphatases (Calf intestinal alkaline phosphatase, TAP and ECAP) was also performed. The conservation of active and binding sites and sequence identity between ECAP, TAP and selected sequences were performed by AlignX tool of VectorNTI platform. The signal peptide of the selected sequence was determined with SignalP tool (XPasy).

6. Cloning of the selected sequence

The pRSETB vector with Ampicillin resistance was selected for the desirable cloning of selected sequence (APT110a, alkaline phosphatase gene from TAB110a). A set of primers were designed based on the restriction sites for the appropriate cloning. Two forward primers (one for the sequence with the signal peptide and one for the sequence without signal peptide) were designed based on an NdeI restriction site, and a reverse primer was also designed based on a BglII restriction site (underlined) (Table 1). Some extra nucleotides were added at the 5’ end for a more sufficient digestion with the corresponding enzymes.

Table 1 : Oligonucleotide (primers) sequences for DNA amplification. FAP1.1: forward primer for APT110a(w) gene, FAP2.1: forward primer for APT110a(w/o) gene, RAP1.1: reverse primer for both APT110a(w) and APT110a(w/o) genes.

	Name	Sequence (5→3)
Forward 1	FAP1.1	CAAAACACATATGTTGCAGCCTGTTTCCC
Forward 2	FAP2.1	CAAACACATATGGATGAGACGCCGGCC
Reverse	RAP1.1	GGAAGATCTTTACTTGATCGCCATGGCG

Two PCR reaction were performed by Phusion® High Fidelity DNA Polymerase (NEB) in order to amplify the two different products (with and without signal peptide) with the following conditions: 1X Phusion HF Buffer, 0.2mM of each dNTP, 12.5pmol of each primer, 50ng of genomic DNA from TAB110a, 1 unit of Phusion polymerase in a final volume 50μl. The PCR schedule consisted of 30s at 98^{o}C followed by 30 cycles of 98^{o}C for 10s, 65^{o}C for 30s and 72^{o}C for 45s. The final extension step was at 72^{o}C for 10 min.

Digestion reactions of the pRSETB plasmid and the two amplified DNA genes were performed as follows: 1X High Buffer, 50 units of NdeI, 30 units of BglII, 100μg/ml BSA and 1.9μg of plasmid DNA and 3μg of amplified DNA genes, respectively, to a final volume of 50μl. The conditions of the digestion were 3.5h at 37^{o}C. After a clean-up assay, 100ng of the plasmid DNA was ligated with the two DNA genes in separate reactions in a ratio 1:3 (plasmid:insert). The reaction conditions were as follows: 1X Ligase Buffer, 10mM ATP, 6 weiss units of T4 DNA Ligase and the appropriate volumes of plasmid DNA and insert in an overnight incubation at 16^{o}C. A reaction only with pRSETB was performed as control. DH5a chemically competent cells were transformed with 5μl of the ligated product (~200ng) based on a heat-shock transformation protocol. The cells were plated on LB-Agar plates with 100μg/ml Ampicillin. The desirable constructs were detected by overnight colony cultures followed by trial digestion with NdeI and BglII restriction enzymes. The enzymes were supplied from MINOTECH Biotechnology (IMBB) and New England Biolabs, Inc.

7. Expression and purification of the desirable constructs

BL21 Star (DE3) pLysS competent cells were transformed by heat-shock with 200ng of pRSETB+APT110a(w) and pRSETB+APT110a(w/o) DNA. The cells were plated on LB-agar plates with 100μg/ml Ampicillin and 25μg/ml Chloramphenicol.

Two colonies [pRSETB+APT110a(w) and pRSETB+APT110a(w/o)] from the above experiment were grown in 75ml LB medium containing 100μg/ml Ampicillin and 25μg/ml Chloramphenicol at 37^{o}C in an overnight incubation. Each culture was used to inoculate 3L of LB-Amp-Chlor. medium and the cultures were grown at 30^{o}C until the 0.4 <A_{600}< 0.6. Afterwards, cultures were, induced at final concentrations with 0.5mM IPTG (isopropyl thio-b-D-galactopyranoside) 10mM $MgSO_4$, 0.4mM $ZnSO_4$ and 10mM KCl and incubated for 4hrs at 25^{o}C. The cells were harvested by centrifugation (12min, 5000g, 4^{o}C) and stored at -20^{o}C.

After a preliminary purification step (using Q-sepharose) of the cells with the two different constructs, cells with pRSETB+APT110a(w) construct were selected due to high protein expression levels in cytoplasmic fraction.

The purification TAP110a alkaline phosphatase is described below. Two grams of frozen cells were thawed in 7ml of 50mM Tris-HCl pH 7.6, 100mM NaCl, 1mM dithiothreitol (DTT) and 0.3mg/ml lysozyme (Resuspension Buffer). After 10 min incubation on ice, the cells were disrupted by 10X (30”sonication, intervals on ice). 1mM phenylmethylsulfonyl fluoride (PMSF) was added during the sonication procedure to inhibit released proteases. The cells were centrifuged at 14.000g for 20 min at 4^{o}C. The supernatant (cytoplasmic fraction) was collected, diluted 5-fold in the Resuspension Buffer and loaded on a Q Sepharose fast flow column (10ml, 1 column volume) (GE Healthcare). The column was equilibrated with buffer containing 25mM Tris-HCl pH 7.6 and 20mM NaCl (buffer A). The elution step was performed by a linear 0-400mM NaCl gradient in buffer A over 15 column volumes by a flow rate 3ml/min and fraction volume of 7.5ml. Alkaline phosphatase activity was detected (by *p*NPP assay) on fractions from 60-200mM NaCl. Detection of relatively pure APT110a protein was tested on an

SDS-PAGE. The fractions ~80-140mM NaCl that exhibited the highest purity were pooled and concentrated with Amicon® Ultra 15 mL centrifugal filter devices to a final volume of 6ml. Purified enzyme was stored at -20^{o}C with 50% glycerol, 1mM $MgCl_2$ and 0.01mM $ZnCl_2$.

Results and Discussion

1. Preliminary screening of bacterial collection strains

A bacterial strain collection, consisting of 262 strains, was screened in order to discover desirable enzymatic activities. The bacterial strains that grew on selected conditions were tested for two enzymatic activities: nuclease and alkaline phosphatase

DNase activity test:

Nuclease activity was demonstrated by using: 1. DNase test agar-methyl green plates and 2. lambda-DNA digestion test. Methyl green is a cation which binds to the negatively-charged DNA. Organisms that produce DNase and grow in an agar medium that contains methyl green-DNA complex, they hydrolyze the DNA and methyl green is released creating a colorless zone around the colony (Kurnick, 1950). Strain samples were divided in two sets for more efficient handling and a third set was created for slow growing strains. Due to the long rest of the bacterial strains at -80^{o}C, cultivation of them was demonstrated at first on LB-agar plates at 8^{o}C and after a visual growth (rise-size), they were transferred on agar-methyl green plates. Strains with no growth were not further tested (dash).

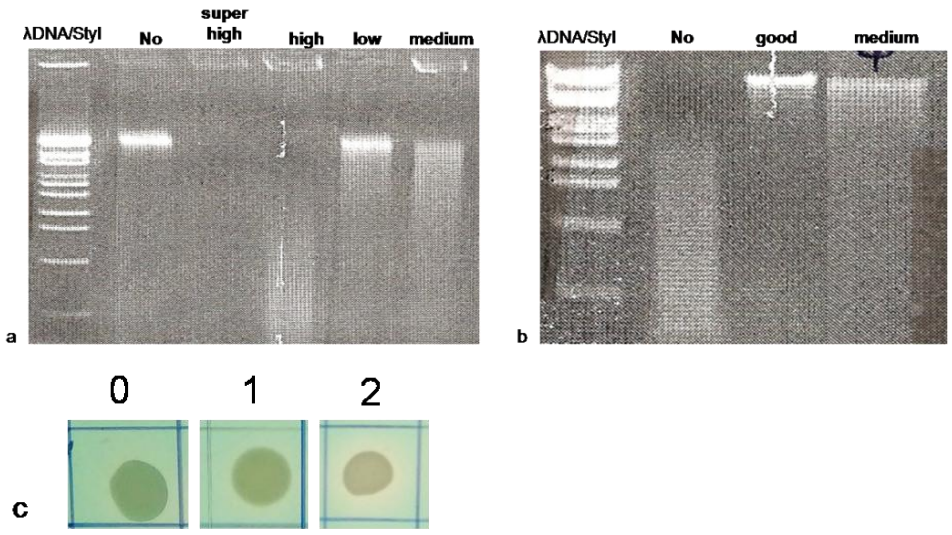

Figure 6: Representative examples of the DNase activity measuring scale. a) Lambda DNA digestion test, b) Lambda DNA digestion test using heat inactivated samples, c) DNase agar test.

A measuring scale, based on the grade of DNase activity, was created. Consequently, characterizations such as, “no”, “low”, “medium”, “high” and “super high” represent the grade of DNase activity. As is obvious, the strains without activity in the lambda DNA digestion test were not tested for heat inactivation as well (dash). Additionally, the “no”, “medium” and “good” characterizations refer to the level of heat inactivation (Figure 6a,b). A counting scale also created about DNase agar test from 0 to 2, depends on the grade of the hyaloids ring on the perimeter of bacteria colony (Figure 6c).

Table 2: SetA. Presentation of nuclease (both lambda DNA digestiont and DNase agar test) activity test of 59 strains.

strain	OD(1/5 dil)	Lambda DNA digestion test	Lambda DNA digestion test (heat inactivation)	DNase agar test
TAB60α	0	–	–	–
TABO	0,716	No	–	1
TAB127	0,249	No	–	0
TAB108a	0,739	super high	No	2
TABN	0,328	high	good	–
TAB102	0,073	low	good	–
TABI	0,432	medium	good	–
TAB116	0,366	medium	good	0
TABT	0,726	No	–	1
TABβ	0,332	No	–	–
TAB103	0,324	No	–	–
TABΦ	0,291	medium	medium	–
TABZ	0,175	No	–	–
TAB110a	0,714	super high	No	2
TABΘ	0,406	high	No	1
TABK	0,13	low	good	–
TAB25	0,223	low	good	–
TAB27	0,411	low	good	–
TAB7	0,015	–	–	–
TAB42	0	–	–	–
TAB44	0,325	No	–	–
TAC116	0,157	No	–	0
TAA95	0,322	No	–	0
TAA13	0,742	No	–	1
TAB126	0,378	No	–	–
TAB119	0,357	No	–	1
TAB121	0,19	No	–	–
TAB114	0,119	No	–	–
TAB93	0	–	–	1

TAB96	0	–	–	–
TAB87	0,012	–	–	–
TAB138	0,016	–	–	–
TAB139	0,198	No	–	–
TAB140	0,319	No	–	–
TAB16	0,33	No	–	–
TAB12	0,048	low	–	0
TAB56	0	–	–	–
TAB50	0,151	No	–	–
TAB106	0,014	–	–	–
TAB107	0	–	–	–
TAB110	0,077	No	–	–
TAB112	0,368	low	good	0
TAB113	0,46	No	–	–
TAB71	0,32	No	control	–
TAE71	0,25	low	good	1
TAE9	0,796	No	control	1
TAE10	0,596	medium	good	1
TAE11	0,469	medium	good	1
TAE12	0,491	low	good	1
TAE13	0,745	No	–	1
TAE14	0,717	No	–	1
TAE15	0,452	low	good	1
TAE16	0,543	No	–	1
TAE2	0,577	No	–	1
TAE3	0,666	low	good	1
TAE4	0,752	low	good	1
TAE6	0,728	low	–	1
TAE7	0,359	low	good	1
TAE8	0,808	low	good	1

As it is clear from Table 2, there are some bacterial strains that have high DNase activity and this activity is inactivated after heating at 65^{o}C for 10 mins. Strains with these characteristics are TABN, TAE10 and TAE 11. Respective bacterial strains from Table 3 with same DNase activity profile are the TAE122, TAE125, TAE126, TAE21, TAE23, TAE18a, TAD1, TAB123, TAE50 and TAE46. Different DNase activity profiles were observed using the two different assays. Typical example is the absence of DNase activity in λDNA digestion test in contrast to high nuclease activity in DNase agar test at TAD7, TAC38, TAE76, TAE77 and TAE78 strains. One possible reason for these opposite observations could be the buffer composition that was used for

λDNA digestion. Different reaction conditions could be tried with the addition of other necessary metals, such as Ca^{2+}, Mn^{2+} and Fe^{2+} for more feasible catalysis conditions.

Table 3: SetB. Presentation of nuclease (both lambda DNA digestion and DNase agar test) activity test of 44 strains.

strain	OD(1/5 dil)	Lambda DNA digestion test	Lambda DNA digestion test (heat inactivation)	DNase agar test
TAE7a	0	–	–	–
TAE62	0,014	–	–	–
TAE122	0,448	high	good	2
TAE125	0,471	high	good	2
TAE126	0,47	high	good	2
TAE127	0,025	–	–	–
TAE21	0,58	high	good	1
TAE23	0,623	high	good	1
TAE24	0,776	medium	–	0
TAE17	0,697	medium	–	1
TAE18a	1,097	high	good	2
TAE34	0,447	medium	–	–
TAA93	0,542	low	–	1
TAA94	0,5	medium	–	1
TAA19	1,038	low	–	2
TAD7	0,221	No	–	2
TAC38	0,395	No	control	2
TAE88	0,725	medium	–	–
TAE85	0,733	medium	–	–
TAC85	0,523	medium	–	–
TAC101;	0,481	No	–	1
TAD1	0,651	high	good	2
TAE90	0,428	medium	–	–
TAA137	0,668	high	No	–
TAD20	0,121	medium	good	–
TAA169	0,49	No	–	–
TAB123	0,187	medium	good	2
TAA149	0,099	No	–	–
TA91	0,31	medium	–	–

TAE76	1,022	No	control	2
TAE77	1,023	No	–	2
TAE78	0,824	No	–	2
TAE54	0,357	medium	–	0
TAE50	0,583	medium	good	2
TAE95	0,385	medium	medium	2
TAE96	0,478	low	–	–
TAE101	0,221	medium	No	1
TAE102	0,169	medium	No	–
TAE48	0,808	medium	–	1
TAE41	0,906	medium	–	2
TAE42	0,891	low	–	2
TAE44	0,309	low	–	–
TAE45	0,083	No	–	–
TAE46	0,069	high	medium	1

In Table 4, slow growing strains in LB agar plates were recultured in liquid LB medium and the respective assays for DNase and alkaline phosphatase activity were performed. Nevertheless, most of them had growth deficiencies and only some had a desirable DNase profile like TAC114 and TAE5 strains. Different DNase activity profiles were also observed using the two different assays, such as high DNase activity in λDNA digestion test in contrast to zero nuclease activity in DNase agar test at TAE5 and TAD5 strains. It could be caused by a stress parameter, like the DNA in the substrate, or by the absence of some supplementary salts and ions like Mg^{2+}, which are necessary for the catalytic mechanism.

Table 4: SetC. Presentation of nuclease (both lambda DNA digestion and DNase agar test) activity test of 67 strains.

strain	OD(1/5 dil)	Lambda DNA digestion test	Lambda DNA digestion test (heat inactivation)	DNase agar test
TAB100	0	–	–	–
TAB101	0,041	No	–	0
TAB9	0,059	No	–	0
TABα	0	–	–	–
TAB59	0	–	–	–

TAC130	0	–	–	–
TAC113	0	–	–	–
TAC124	0,374	No	–	0
TAC126a	0	–	–	–
TAC126b	0	–	–	–
TAC119	0	–	–	–
TAC121	0	–	–	–
TAC122	0,03	–	–	–
TAC113a	0	–	–	–
TAC114	0,539	high	No	1
TAC117	0	–	–	–
TAC112	0	–	–	–
TAC111	0	–	–	–
TAC126	0	–	–	–
TAC123	0	–	–	–
TAC125a	0	–	–	–
TAC140a	0,088	medium	good	2
TAB86	0	–	–	–
TAB51	0	–	–	–
TAB156	0	–	–	–
TAE5	0,972	high	good	0
TAE123	0,047	medium	–	0
TAE124	0,391	medium	–	0
TAE120	0	–	–	–
TAA10	0,428	medium	–	0
TAA61	0,26	medium	–	0
TAD176	0	–	–	–
TAC97	0,063	No	–	–
TAC36	0	–	–	–
TAC43	0,097	No	–	–
TAC2	0,188	No	–	0
TAC1	0	–	–	–
TAC95a	0,096	No	–	0
TAC104mc	0,414	No	–	0
TAC96mo	0,046	No	–	–
B10	0,253	No	–	0
A5	0,176	No	–	–
TA39	0	–	–	–
TA41	0	–	–	–
TAE87	0,173	No	–	0
TAE84	0,583	medium	–	0
TAE83	0,287	No	–	0
TAD5	1.059	super high	No	0
TAE123	0,038	No	–	–
TA64	0,313	medium	–	0
TA70	0,151	No	–	–
TAA145	0,299	medium	–	0

TAE79	0,529	medium	–	1
TAE49	0	–	–	–
TAE98	0,05	No	–	–
TAE99	0,094	No	–	–
TAE100	0,33	No	–	–
TAE94	0,145	No	–	–
TAE81	0,386	No	–	–
TAE82	0,552	No	–	0
TAE86	0,029	No	–	–
TAE107	0,404	No	–	0
TAE108	0,387	No	–	0
TAE47	0,059	No	–	–
TAE43	0	–	–	–
TAA20	0,758	No	–	1
TAE75	0,467	No	–	0

Alkaline phosphatase activity test:

Alkaline phosphatase activity was demonstrated using the *p*NPP (*p*-Nitrophenyl-Phosphate) assay. *p*NPP is a chromogenic non-specific substrate, for alkaline and acid phosphatase activity detection. The activity is measured based on the absorbance of 4-Nitrophenol, a chromogenic product derived from the hydrolysis of *p*NPP by the action of alkaline phosphatase. Heat inactivated samples were also assayed in order to evaluate the inhibition of alkaline phosphatase activity. Any detected absorbance up to 10% higher than background was characterized as non-significant.

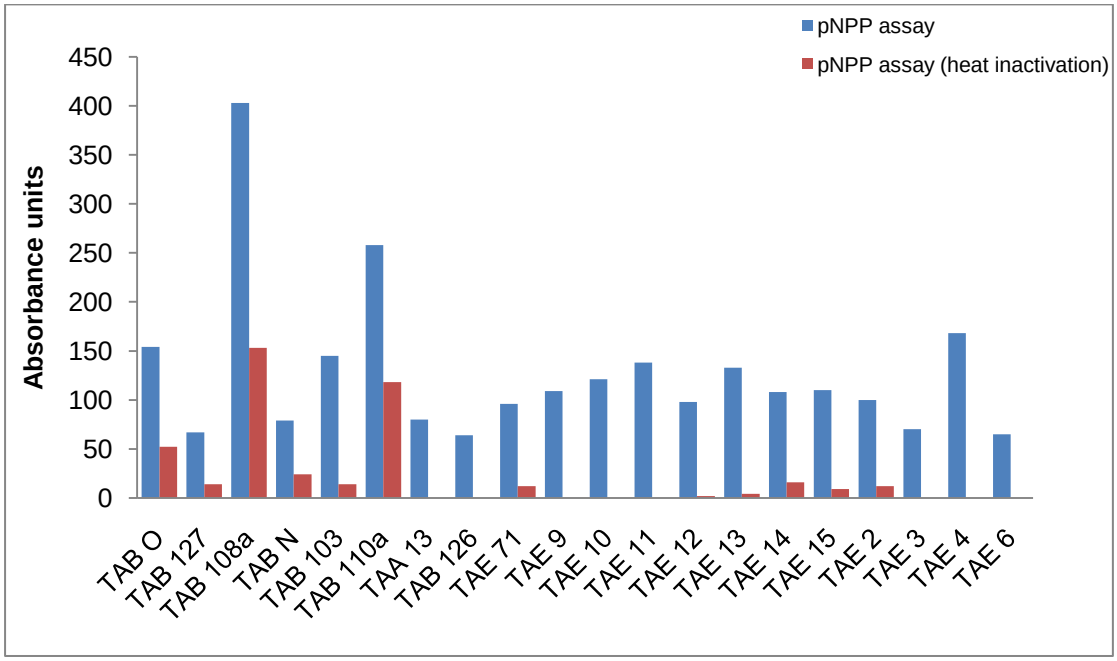

Figure 7: Representation of Absorbance units in *p*NPP assay before (blue) and after (red) heat inactivation samples from setA.

Regarding *p*NPP assay data, bacterial strains of SetA with a desirable profile are the TAB108a, TAB110a and TAE 4 (Figure 7) and TAE23, TAE24, TAE17, TAE34, TAA93, TAD7, TAE90, TAA149, TAE77, TAE78, TAE54, TAE95, TAE41, TAE42 and TAE44 from SetB (Figure 8). Strains with a desirable phosphatase activity profile from setC are TAE5 and TAD5 (Figure 9).

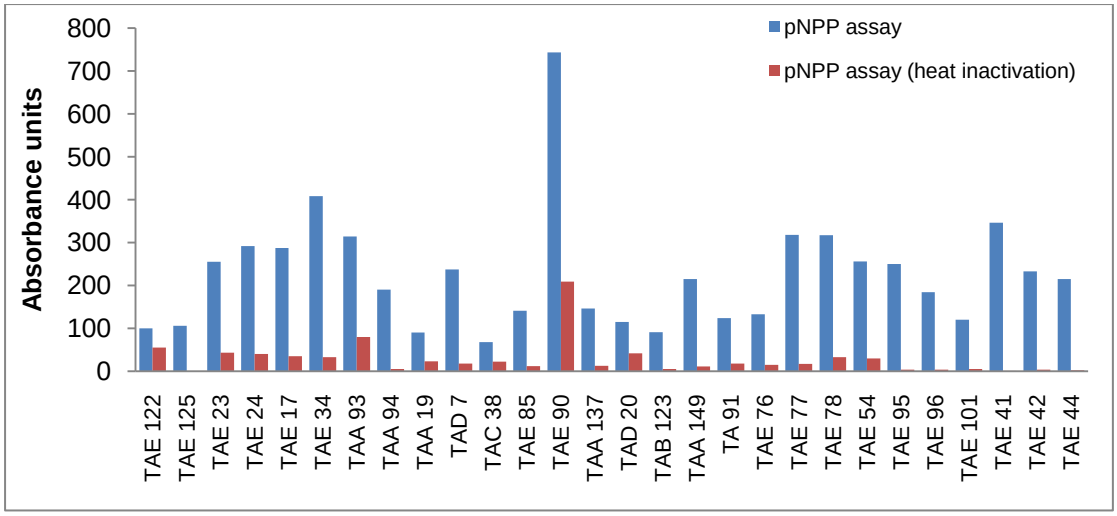

Figure 8: Representation of Absorbance units in *p*NPP assay before (blue) and after (red) heat inactivation samples from setB.

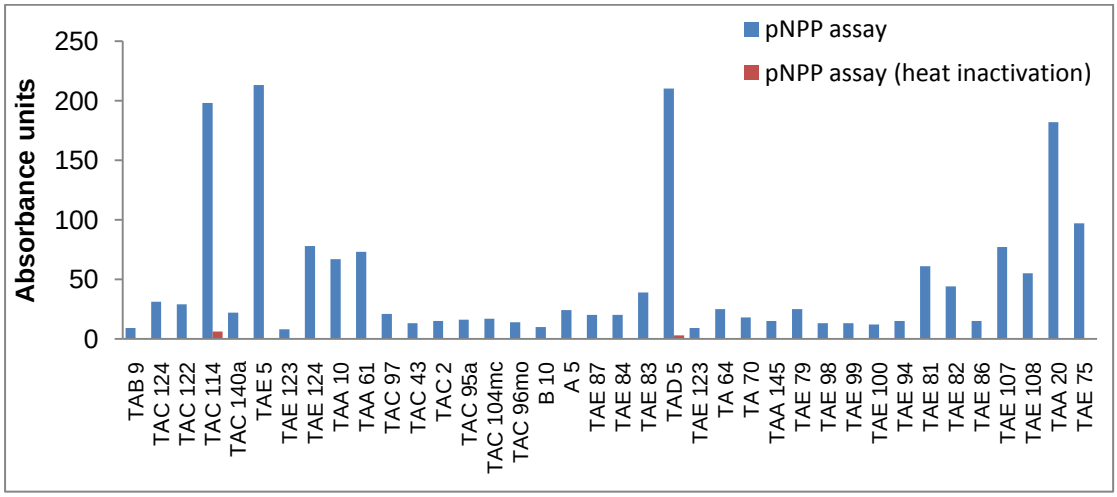

Figure 9: Representation of Absorbance units in *p*NPP assay before (blue) and after (red) heat inactivation from setC.

Comparison of nuclease and alkaline phosphatase tests resulted in the selection of nine strains for further analysis. Genomic DNA samples from TAB108a, TAB110a, TAE23, TAE5, TAE122, TAE125, TAE126, TAD1 and TAD7 strains were isolated for DNA sequencing.

The number of reads and the number of contigs are represented on Table 5 after the *de novo* assembly by Genomics Facility (IMBB). The estimated closest neighbors, based on the RAST platform (Rapid Annotation using Subsystem Technology), revealed that all strains may belong to some

genus (*Pseudomonas, Serratia, Rahnella, Carnobacterium)* containing psychrophilic species.

Table 5: *De novo* assembly by Genomics Facility. Closest neighbors by RAST platform.

Sample No	Sample name	No of reads Proton	Read length	No of contigs (*De novo* assembly)	N50 (contigs)	Average coverage	Closest neighbors	% similarity
1	TAB108a	9,398,514	195 bp	269	208666	300	*Pseudomonas fluorescens* PfO-1	72.89%
2	TAB110a	9,773,174	197 bp	297	413040	355	*Serratia proteamaculans* 568	82.18%
3	TAE23	6,999,366	204 bp	3,980	9,681	136	*Pseudomonas psychrophila* HA-4	-
4	TAE5	6,618,998	197 bp	2097	18047	136	*Pseudomonas psychrophila* HA-4	-
5	TAE122	7,736,367	186 bp	181	167353	242	*Pseudomonas fluorescens* PfO-1	69.53%
6	TAE125	9,100,994	197 bp	294	164792	300	*Pseudomonas fluorescens* PfO-1	70.31%
7	TAE126	7,939,833	200 bp	371	188169	261	*Pseudomonas fluorescens* PfO-1	70.32%
8	TAD1	10,410,090	190 bp	1831	437054	314	*Rahnella* sp. Y9602	71.23%
9	TAD7	11,109,249	194 bp	5219	19282	182	*Carnobacterium* sp. AT7	-

2. Selection of a desirable alkaline phosphatase gene

In order to identify alkaline phosphatase related sequences the sequencing data were screened against commercial alkaline phosphatase amino acid sequences (Calf Intestinal Phosphatase, ECAP (*E.coli*) and TAP),

Evaluation of the best hits related to commercial alkaline phosphatase protein sequences showed that No.2624 gene of TAB110a (coding respective protein APT110a) strain has the highest identity with them. The No.2624 gene displays 27.55% identity with Calf intestinal Alkaline Phosphatase gene, 30.47% identity with from TAB5 strain (TAP) and 75.64% identity with APase of *E.coli* (ECAP). The length of the translated gene No.2624 is 475 amino acids (Table 6).

Table 6: Best Alignment hits by correlation of Calf Intestinal Phosphatase, ECAP (*E.coli*) and TAP (Antarctic phosphatase) with amino acid sequences from the sequenced bacterial strains.

Query sequence	subject sequence	% identity	Alignment length (aa)	E-value
Calf Intestinal Alkaline Phosphatase	TAB110a_gene2624_475aa	27.55	490	3.00E-25
ECAP	TAB110a_gene2624_475aa	75.64	472	0.0
TAP	TAB110a_gene2624_475aa	30.47	407	2.00E-36

Alignment of the amino acid sequences of No.2624 (TAB110a), ECAP and TAP genes, showed significant conservation at the active and metal binding site residues (Table 7). Differences are also observed in two residues. The lysine in position 354 and the aspartic acid in position 179 of APT110a correspond to a thryptophan and histidine in the respective positions of TAP. A previous study revealed that the triple mutant (W260K/A219N/H135D) of TAP results in an enzyme with similar E_a with the wild type that reflects its psychrophilic character. However, the triple mutant is more stable than the wild type due to the His→Asp substitution (Tsigos *et al.*, 2001) . The same substitutions in the corresponding residues are observed in the APT110a gene, suggesting that there is a possibility for a psychrophilic activity. However, exactly the same substitutions are observed in ECAP, a mesophilic

enzyme. Further experimentation could elucidate the occurrence of psychrophilicity in APT110a.

Analysis of the amino acid composition of APT110a revealed a lower number of proline residues (18 instead of 21 in *E.coli*), a characteristic of the adaptation mechanism of some psychrophiles (Sakaguchi *et al.*, 2006). Although, the *APT110a* gene is considerably identical to ECAP gene (~73.1% identity based on AlignX tool), and presents only 25.2% identity with the TAP, further analysis will follow.

Table 7: Conserved active and metal binding residues between TAP, ECAP, AP gene of TAB110a. TAP:Antarctic Phosphatase, ECAP: Alkaline phosphatase from *E.coli.*

Active and metal binding sites	TAP	ECAP	AP gene of TAB110a strain
	D83	D123	D127
	W260	**K350**	**K354**
	R148	R205	R209
	Y325	K415	K419
M1 (Zn)	D259	D349	D353
	H263	H353	H357
	H337	H434	H438
M2 (Zn)	D43	D73	D77
	S84	S124	S128
	D301	D391	D395
	H302	H392	H396
M3 (Mg)	D43	D73	D77
	H135	**D175**	**D179**
	T137	T177	T181
	E254	E344	E348

Analysis for the presence of signal peptide in APT110a amino acid sequence (475aa) was examined by SignalP (ExPasy). The predicted cleavage site for the putative signal peptide is near the N-terminus between A23 and D24 residues and should be necessary for cytoplasmic membrane translocation. TAP protein bears a signal peptide between S22 and V23 residues (Figure 10) (Rina *et al.*, 2000).

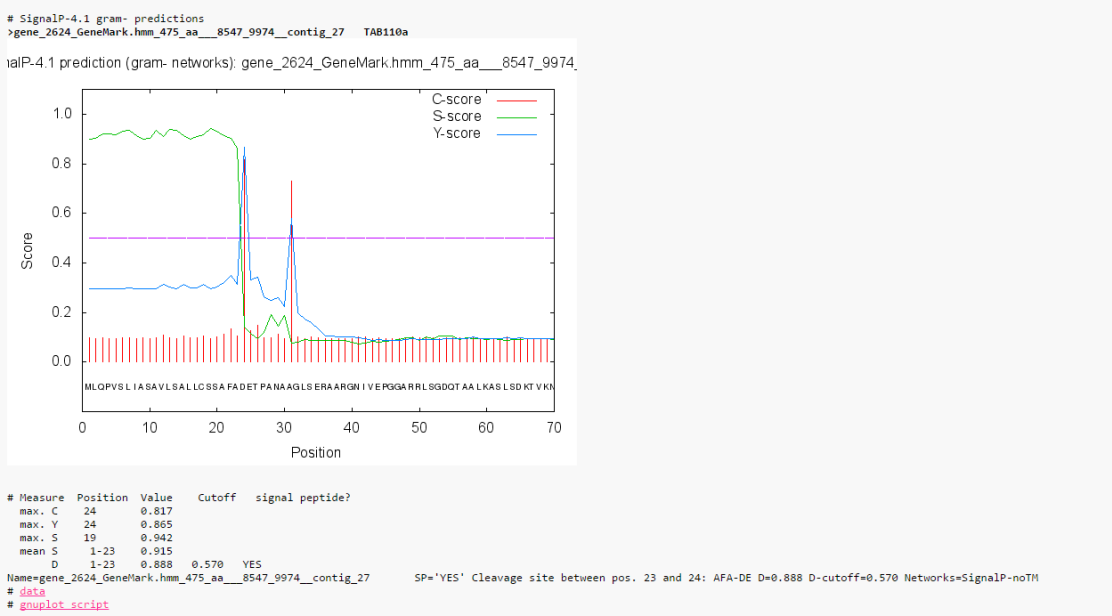

Figure 10: The predicted cleavage site for the putative signal peptide (between A23 and D24) of APT110a by SignalP (ExPasy).

3. Cloning of the selected gene encoding alkaline phosphatase, *APT110a*

Two sequences of APT110a gene were synthesized by PCR (with and without signal peptide sequence). The purified products with length 1428bp (gene with signal peptide) and 1359bp (gene without signal peptide) were ligated to pRSETB as previously described. The two constructed plasmid bearing gene with signal peptide and gene without signal peptide [APT110a(w) and APT110a(w/o) respectively] were transformed to BL21 Star (DE3) pLysS *E.coli* strain for heterologous expression of the desired genes

Cell samples after induction were lysed and analyzed by SDS PAGE. Both proteins are expressed at high levels (APT110a(w) and APT110a(w/o) estimated molecular weights are 49.696 and 47.421 Da respectively) and most of them is located at the cytoplasmic fraction. Triton X-100 treatment was also performed in order to check the existence of alkaline phosphatase protein on membranes (Figure 11).

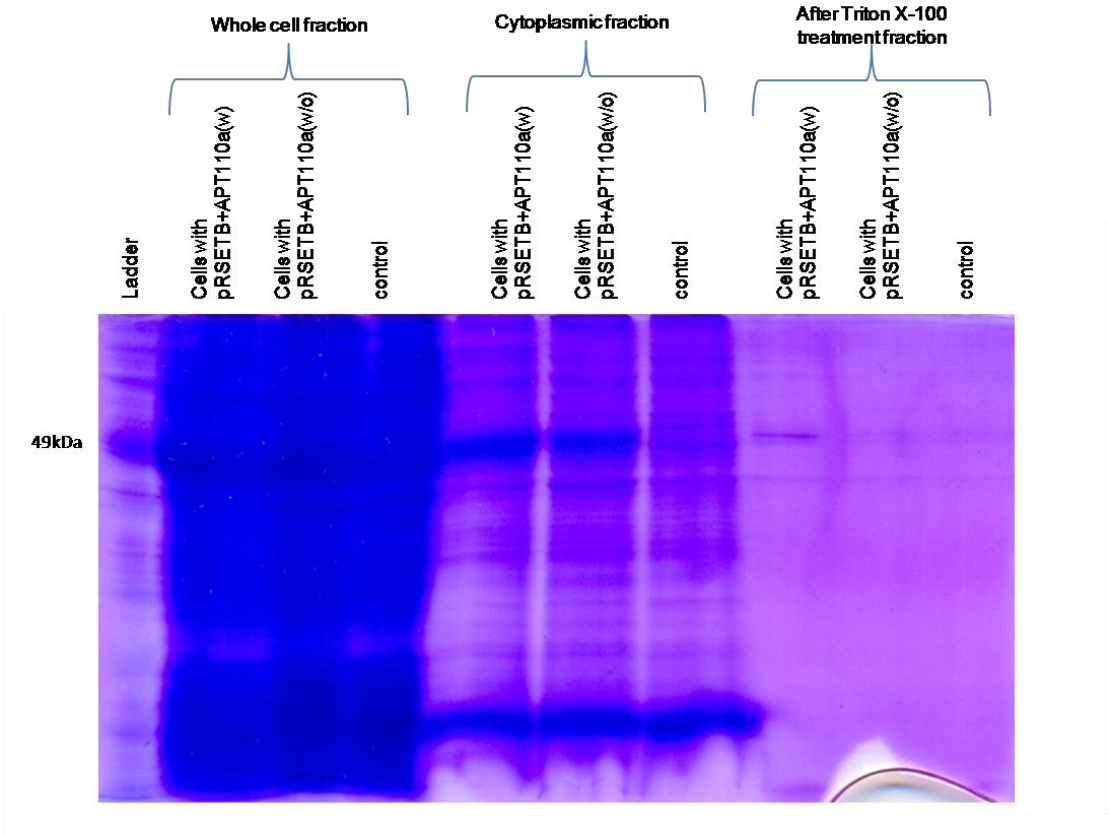

Figure 11: Protein molecular weight representation of transformed BL21 Star (DE3) pLysS *E.coli*

cells with pRSETB+ APT110a(w) and pRSETB+ APT110a(w/o) by different cell fractions (whole cell, cytoplasmic, after Triton X-100 treatment). Transformed BL21 Star (DE3) pLysS *E.coli* cells with only pRSETB were used as control.

*p*NPP assays on the cytoplasmic fragment of the two proteins showed that APT110a(w) exhibits considerably higher activity than APT110a(w/o) which proves the essential role of the signal peptide to the activity of the enzyme. Cytoplasmic fraction of APT110a(w) was further purified using ion exchange chromatography (Q Sepharose ff). Elution of alkaline phosphatase protein was achieved by a linear gradient of NaCl. As shown in Figure 12, the fraction with the highest amount of APT110a was detected from 100-140mM NaCl. The activity of the alkaline phosphatase protein in elution fractions was also tested by *p*NPP assay; activity was detected between 80mM and 240mM NaCl protein elution fractions.

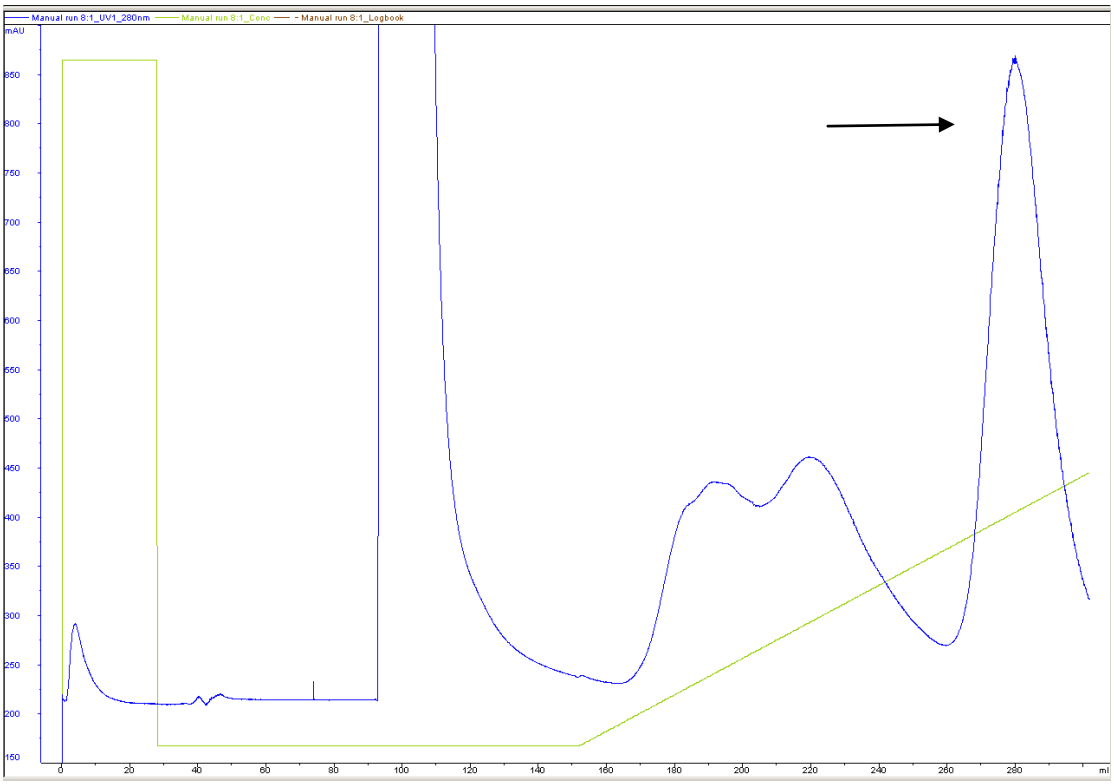

Figure 12: Protein elution with NaCl gradient (0-400mM) using *ÄKTA* protein purification system. The highest pick represents the eluted protein fractions with high alkaline phosphatase activity tested with the *p*NPP assay.

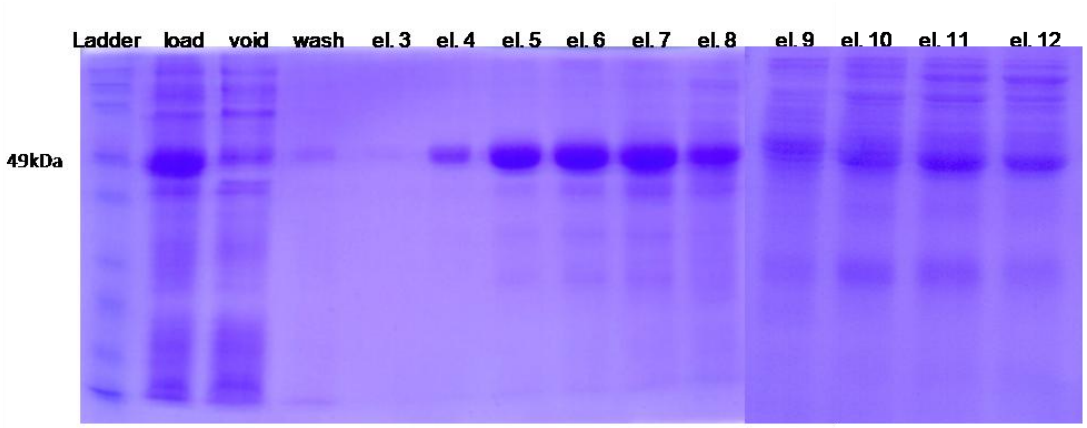

Figure 13: Protein molecular weight representation of the most active elution fractions by Q Sepharose fast flow samples in SDS-PAGE analysis. marker: BenchMark™ Protein Ladder (Invitrogen), el.3: elution with 60mM NaCl, el.4: 80mM NaCl, el.5: 100mM NaCl, el.6: 120mM NaCl, el.7: 140mM NaCl, el.8: 160mM NaCl, el.9: 180mM NaCl, el.10: 200mM NaCl, el.11: 220mM NaCl, el.12: 240mM NaCl.

The SDS-PAGE in Figure 13 verifies the existence of the alkaline phosphatase in the elution fractions. Only the fractions from 4 to 7 were pooled, due to the high abundance of APT110a(w) protein. The remaining fractions also contained high expression levels of the proteins, but they were rejected due to the appearance of other protein populations. An additional chromatography step for higher percentage of protein purity should follow.

Future perspectives

Having a high purity level of protein, characterization of the putative psychrophilic character of APT110a needs to be carried out. High catalytic activity at low or moderate temperature and remarkable thermal instability are the enzymatic properties that we hope to identify. For the former, the *p*NPP assay could be used in order to elucidate the optimal temperature and pH of the enzyme activity, by measuring the absorbance of *p*-nitrophenol using a sprectrophotometer. Different substrate (*p*NPP) concentrations will be used for the determination of the kinetic parameters (k_{cat}, K_m). Catalytic efficiency will be compared with other psychrophilic commercial alkaline phosphatases such as AnP and SAP. In order to examine the potential thermal instability of the enzyme, heat inactivation need to be assayed in a temperature range. Samples from different time intervals could be tested for the residual activity based on the standard assay. Furthermore, differential scanning calorimetry will be a useful method to study the thermal stability of our target enzyme.

Additionally, due to the necessity of divalent cations for the catalytic mechanism of alkaline phosphatases, examination of the metal specificity could follow. Phosphatase activity could be tested by dialysis of the enzyme in solutions with different compositions of divalent cations, like Zn^{2+}, Mg^{2+}, Co^{2+} and Ca^{2+}.

However, a common use of alkaline phosphatase in molecular biology is the dephosphorylation of plasmid DNA prior cloning in order to prevent recircularization. Determination of this potential application could be elucidated by using as substrates digested plasmids with restriction endonucleases which create: a) 3’ protruding cohesive, b) 5’ protruding cohesive and c) blunt ends. Dephosphorylation efficiency can be measured based on the CFU (colony forming unit) of transformed cells with ligated plasmids. A control with nondephosphorylated plasmids need to be also used.

Further studies and correlation with other commercial alkaline phosphatases could elucidate its potential use in molecular biology applications.

Bibliography

Aghajari, N., Feller, G., Gerday, C., and Haser, R. (1998) Structures of the psychrophilic Alteromonas haloplanctis alpha-amylase give insights into cold adaptation at a molecular level. *Structure* **6**: 1503–16.

Aghajari, N., Van Petegem, F., Villeret, V., Chessa, J.-P., Gerday, C., Haser, R., and Van Beeumen, J. (2003) Crystal structures of a psychrophilic metalloprotease reveal new insights into catalysis by cold-adapted proteases. *Proteins* **50**: 636–47.

Baldwin, R.L. (2008) The search for folding intermediates and the mechanism of protein folding. *Annu. Rev. Biophys.* **37**: 1–21.

Bjelic, S., Brandsdal, B.O., and Aqvist, J. (2008) Cold adaptation of enzyme reaction rates. *Biochemistry* **47**: 10049–57.

Bowman, J.P. (2008) Genomic Analysis of Psychrophilic Prokaryotes. In, *Psychrophiles: from Biodiversity to Biotechnology*. Springer Berlin Heidelberg, Berlin, Heidelberg, pp. 265–284.

Buzzini, P., Branda, E., Goretti, M., and Turchetti, B. (2012) Psychrophilic yeasts from worldwide glacial habitats: diversity, adaptation strategies and biotechnological potential. *FEMS Microbiol. Ecol.* **82**: 217–241.

Cavicchioli, R. (2006) Cold-adapted archaea. *Nat. Rev. Microbiol.* **4**: 331–343.

Collins, T., Meuwis, M.-A., Gerday, C., and Feller, G. (2003) Activity, stability and flexibility in glycosidases adapted to extreme thermal environments. *J. Mol. Biol.* **328**: 419–28.

Cootes, T.F., Twining, C., Limited, I., and Rodriguez, P.E.L. (2009) (12) United States Patent. **2**:.

Cowan, J.A. (2002) Structural and catalytic chemistry of magnesium-dependent enzymes. *Biometals* **15**: 225–35.

D'Amico, S., Gerday, C., and Feller, G. (2003) Temperature adaptation of proteins: engineering mesophilic-like activity and stability in a cold-

adapted alpha-amylase. *J. Mol. Biol.* **332**: 981–8.

D'Amico, S., Marx, J.-C., Gerday, C., and Feller, G. (2003) Activity-stability relationships in extremophilic enzymes. *J. Biol. Chem.* **278**: 7891–6.

Davail, S., Feller, G., Narinx, E., and Gerday, C. (1994) Cold adaptation of proteins. Purification, characterization, and sequence of the heat-labile subtilisin from the antarctic psychrophile Bacillus TA41. *J. Biol. Chem.* **269**: 17448–53.

Feller, G. (2013) Psychrophilic enzymes: from folding to function and biotechnology. *Scientifica (Cairo).* **2013**:.

Feller, G., d'Amico, D., and Gerday, C. (1999) Thermodynamic stability of a cold-active alpha-amylase from the Antarctic bacterium Alteromonas haloplanctis. *Biochemistry* **38**: 4613–9.

Feller, G. and Gerday, C. (2003) Psychrophilic enzymes: hot topics in cold adaptation. *Nat. Rev. Microbiol.* **1**: 200–8.

Feller, G. and Gerday, C. (1997) Psychrophilic enzymes: molecular basis of cold adaptation. *Cell. Mol. Life Sci.* **53**: 830–41.

Feller, G., Payan, F., Theys, F., Qian, M., Haser, R., and Gerday, C. (1994) Stability and structural analysis of alpha-amylase from the antarctic psychrophile Alteromonas haloplanctis A23. *Eur. J. Biochem.* **222**: 441–7.

Fields, P.A. and Somero, G.N. (1998) Hot spots in cold adaptation: localized increases in conformational flexibility in lactate dehydrogenase A4 orthologs of Antarctic notothenioid fishes. *Proc. Natl. Acad. Sci. U. S. A.* **95**: 11476–81.

Georlette, D., Damien, B., Blaise, V., Depiereux, E., Uversky, V.N., Gerday, C., and Feller, G. (2003) Structural and functional adaptations to extreme temperatures in psychrophilic, mesophilic, and thermophilic DNA ligases. *J. Biol. Chem.* **278**: 37015–23.

Gianese, G., Bossa, F., and Pascarella, S. (2002) Comparative structural analysis of psychrophilic and meso- and thermophilic enzymes. *Proteins*

47: 236–49.

Giver, L., Gershenson, A., Freskgard, P.O., and Arnold, F.H. (1998) Directed evolution of a thermostable esterase. *Proc. Natl. Acad. Sci. U. S. A.* **95**: 12809–13.

Gounot, A.-M. (1991) Bacterial life at low temperature: physiological aspects and biotechnological implications. *J. Appl. Bacteriol.* **71**: 386–397.

HORIUCHI, T., HORIUCHI, S., and MIZUNO, D. (1959) A Possible Negative Feedback Phenomenon controlling Formation of Alkaline Phosphomonoesterase in Escherichia coli. *Nature* **183**: 1529–1530.

Hsia, K.-C., Li, C.-L., and Yuan, H.S. (2005) Structural and functional insight into sugar-nonspecific nucleases in host defense. *Curr. Opin. Struct. Biol.* **15**: 126–34.

Hulett, F.M., Kim, E.E., Bookstein, C., Kapp, N. V, Edwards, C.W., and Wyckoff, H.W. (1991) Bacillus subtilis alkaline phosphatases III and IV. Cloning, sequencing, and comparisons of deduced amino acid sequence with Escherichia coli alkaline phosphatase three-dimensional structure. *J. Biol. Chem.* **266**: 1077–84.

Jung, S.-K., Jeong, D.G., Lee, M.S., Lee, J.-K., Kim, H.-K., Ryu, S.E., et al. (2008) Structural basis for the cold adaptation of psychrophilic M37 lipase from Photobacterium lipolyticum. *Proteins* **71**: 476–84.

Jung, Y.H., Yi, J.-Y., Jung, H.J., Lee, Y.K., Lee, H.K., Naicker, M.C., et al. (2010) Overexpression of cold shock protein A of Psychromonas arctica KOPRI 22215 confers cold-resistance. *Protein J.* **29**: 136–42.

Koutsioulis, D., Wang, E., Tzanodaskalaki, M., Nikiforaki, D., Deli, A., Feller, G., et al. (2008) Directed evolution on the cold adapted properties of TAB5 alkaline phosphatase. *Protein Eng. Des. Sel.* **21**: 319–27.

Kurnick, N.B. (1950) The determination of desoxyribonuclease activity by methyl green; application to serum. *Arch. Biochem.* **29**: 41–53.

Lonhienne, T., Mavromatis, K., Vorgias, C.E., Buchon, L., Gerday, C., and

Bouriotis, V. (2001) Cloning, sequences, and characterization of two chitinase genes from the Antarctic Arthrobacter sp. strain TAD20: isolation and partial characterization of the enzymes. *J Bacteriol* **183**:.

Maguire, M.E. and Cowan, J.A. (2002) Magnesium chemistry and biochemistry. *Biometals* **15**: 203–10.

Margesin, R., Neuner, G., and Storey, K.B. (2007) Cold-loving microbes, plants, and animals--fundamental and applied aspects. *Naturwissenschaften* **94**: 77–99.

Mavromatis, K., Tsigos, I., Tzanodaskalaki, M., Kokkinidis, M., and Bouriotis, V. (2002) Exploring the role of a glycine cluster in cold adaptation of an alkaline phosphatase. *Eur. J. Biochem.* **269**: 2330–5.

McComb, R.B., Bowers, G.N., and Posen, S. (1979) Alkaline Phosphatase Springer US, Boston, MA.

Medigue, C., Krin, E., Pascal, G., Barbe, V., Bernsel, A., Bertin, P.N., et al. (2005) Coping with cold: the genome of the versatile marine Antarctica bacterium Pseudoalteromonas haloplanktis TAC125. *Genome Res.* **15**: 1325–1335.

Morgan-Kiss, R.M., Priscu, J.C., Pocock, T., Gudynaite-Savitch, L., and Huner, N.P.A. (2006) Adaptation and acclimation of photosynthetic microorganisms to permanently cold environments. *Microbiol. Mol. Biol. Rev.* **70**: 222–52.

Morita, R.Y. (1975) Psychrophilic Bacteria1. *BACrERIOLOGICAL Rev.* **39**: 144–167.

Murphy, J.E. and Kantrowitz, E.R. (1994) Why are mammalian alkaline phosphatases much more active than bacterial alkaline phosphatases? *Mol. Microbiol.* **12**: 351–7.

Murphy, J.E., Xu, X., and Kantrowitz, E.R. (1993) Conversion of a magnesium binding site into a zinc binding site by a single amino acid substitution in Escherichia coli alkaline phosphatase. *J. Biol. Chem.* **268**: 21497–500.

Papaleo, E., Pasi, M., Tiberti, M., and De Gioia, L. (2011) Molecular Dynamics of Mesophilic-Like Mutants of a Cold-Adapted Enzyme: Insights into Distal Effects Induced by the Mutations. *PLoS One* **6**: e24214.

Paredes, D.I., Watters, K., Pitman, D.J., Bystroff, C., Dordick, J.S., D'Amico, S., et al. (2011) Comparative void-volume analysis of psychrophilic and mesophilic enzymes: Structural bioinformatics of psychrophilic enzymes reveals sources of core flexibility. *BMC Struct. Biol.* **11**: 42.

Piette, F., D'Amico, S., Struvay, C., Mazzucchelli, G., Renaut, J., Tutino, M.L., et al. (2010) Proteomics of life at low temperatures: trigger factor is the primary chaperone in the Antarctic bacterium Pseudoalteromonas haloplanktis TAC125. *Mol. Microbiol.* **76**: 120–32.

Rentier-Delrue, F., Mande, S.C., Moyens, S., Terpstra, P., Mainfroid, V., Goraj, K., et al. (1993) Cloning and overexpression of the triosephosphate isomerase genes from psychrophilic and thermophilic bacteria. Structural comparison of the predicted protein sequences. *J. Mol. Biol.* **229**: 85–93.

Rina, M., Pozidis, C., Mavromatis, K., Tzanodaskalaki, M., Kokkinidis, M., and Bouriotis, V. (2000) Alkaline phosphatase from the Antarctic strain TAB5. Properties and psychrophilic adaptations. *Eur. J. Biochem.* **267**: 1230–8.

Rodrigues, D.F. and Tiedje, J.M. (2008) Coping with Our Cold Planet. *Appl. Environ. Microbiol.* **74**: 1677–1686.

Saelensminde, G., Halskau, Ø., and Jonassen, I. (2009) Amino acid contacts in proteins adapted to different temperatures: hydrophobic interactions and surface charges play a key role. *Extremophiles* **13**: 11–20.

Sakaguchi, M., Matsuzaki, M., Niimiya, K., Seino, J., Sugahara, Y., and Kawakita, M. (2006) Role of Proline Residues in Conferring Thermostability on Aqualysin I. *J. Biochem.* **141**: 213–220.

Sandsdalen, E., Stenberg, E., Application, F., and Data, P. (2003) (12) United States Patent. **2**:.

Sarmiento, F., Peralta, R., and Blamey, J.M. (2015) Cold and Hot Extremozymes: Industrial Relevance and Current Trends. *Front. Bioeng. Biotechnol.* **3**: 148.

Schultz, C.P. (2000) Illuminating folding intermediates. *Nat. Struct. Biol.* **7**: 7–10.

Siddiqui, K.S., Poljak, A., Guilhaus, M., De Francisci, D., Curmi, P.M.G., Feller, G., et al. (2006) Role of lysine versus arginine in enzyme cold-adaptation: modifying lysine to homo-arginine stabilizes the cold-adapted alpha-amylase from Pseudoalteramonas haloplanktis. *Proteins* **64**: 486–501.

Smalås, A.O., Heimstad, E.S., Hordvik, A., Willassen, N.P., and Male, R. (1994) Cold adaption of enzymes: structural comparison between salmon and bovine trypsins. *Proteins* **20**: 149–66.

Smalas, A.O., Leiros, H.K., Os, V., and Willassen, N.P. (2000) Cold adapted enzymes. *Biotechnol Annu Rev* **6**:.

Tsigos, I., Mavromatis, K., Tzanodaskalaki, M., Pozidis, C., Kokkinidis, M., and Bouriotis, V. (2001) Engineering the properties of a cold active enzyme through rational redesign of the active site. *Eur. J. Biochem.* **268**: 5074–5080.

Wang, E., Koutsioulis, D., Leiros, H.-K.S., Andersen, O.A., Bouriotis, V., Hough, E., and Heikinheimo, P. (2007) Crystal structure of alkaline phosphatase from the Antarctic bacterium TAB5. *J. Mol. Biol.* **366**: 1318–31.

Wintrode, P.L. and Arnold, F.H. (2000) Temperature adaptation of enzymes: lessons from laboratory evolution. *Adv. Protein Chem.* **55**: 161–225.

Yang, W. (2011) Nucleases: diversity of structure, function and mechanism. *Q. Rev. Biophys.* **44**: 1–93.